Quantum Energy Teleportation across Multi-Qubit Systems using W-State Entanglement

Alif Elham Khan[a,*], Humayra Anjum[a], Mahdy Rahman Chowdhury[a]

[a]*Department of Electrical and Computer Engineering,
North South University, Dhaka, 1229, Bangladesh*

Abstract

Quantum-energy teleportation (QET) has so far only been realized on a two-qubit platform. Real-world communication, however, typically involves multiple parties. Here we design and experimentally demonstrate the first multi-qubit QET protocol using a robust W-state multipartite entanglement. Three-, four-, and five-qubit circuits were executed both on noiseless simulators and on IBM superconducting hardware. In every case a single sender injects an energy E_0 that is then deterministically and decrementally harvested by several remote receivers, confirming that energy introduced at one node can be redistributed among many entangled subsystems at light-speed-limited classical latency. Our results open a practical route toward energy-aware quantum networks.

*Keywords:* **QET**, **W-state Entanglement**, **Multi-Qubit**, **Energy Transfer**

1. Introduction

Quantum Energy Teleportation (QET) is a protocol that aims to achieve successful energy transportation via local operations and classical communication without breaking any known physical laws [1] [2]. Since its proposal in the year 2008, it has become the focus of studies and trials. The methodology entails using local operations that rely on data from a remote measurement to extract zero-point energy from entangled many-body systems [3]. More than a decade later, the first demonstration of QET has taken place

---

*E-mail: alif.khan1@northsouth.edu

on real quantum hardware [4] [5]. The experiment, run on a two-qubit circuit, has surpassed the boundaries of large distances by transporting energy much faster than the time scale of heat generation in the natural time evolution. However, to truly leverage the power of long-distance quantum energy teleportation, we must investigate the feasibility of QET across multi-qubit systems because exchanging energy between multiple subsystems is more natural. In this study, we devised a quantum circuit employing W-state multipartite entanglement to observe energy transfer behavior across multiple entangled qubits. It is essential to understand that QET does not promise to
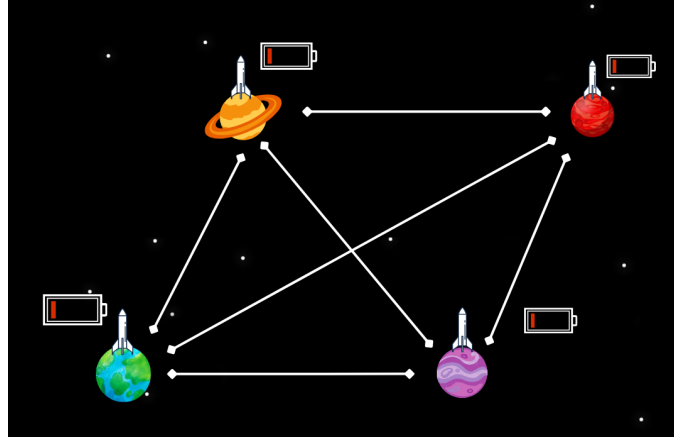
(a) Before injecting energy
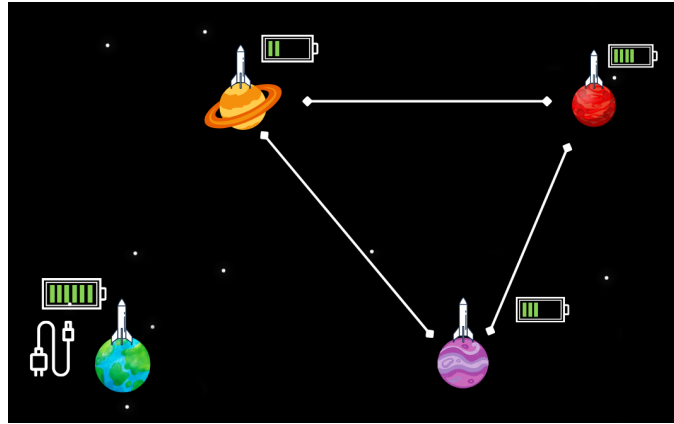
(b) After injecting energy

Figure 1: (a) Entanglement exists between a sender and three receivers, but energy has not yet been injected. (b) Energy injected into the sender's system is instantly distributed to the receivers located at far-off locations using Multi-Qubit Quantum Energy Teleportation.

2

create energy out of a vacuum. Instead, energy can be unlocked using knowledge from a sender with energy in a far-off location. From this perspective, QET looks less like energy creation and more like the teleportation of energy from one place to another [6]. In line with these conceptual foundations, we have devised a quantum circuit where energy is first injected into one qubit, Alice, and later harvested from the other entangled qubits: Bob, Charlie, Duke, Eric, etc, using the knowledge obtained from Alice. The multipartite entanglement exists in such a way that all of the remaining qubits are entangled to Alice such that when energy is injected into Alice, others can harvest it from far-off locations with the information provided by Alice. All of the participants are entangled using W-state entanglement [7]. So, it is possible to inject energy at any node and harvest it from any other node. Injecting energy into the sender's system ensures that the receivers receive energy much faster than the time scale of heat generation in the natural time evolution. However, the QET protocols are based on local observation and classical communication (LOCC) [8], which limits the protocols to the speed of light because the information on how to harvest the energy is sent through a classical channel bounded by the speed of light.

2. Multiqubit System for QET

QET uses quantum entanglement [9], a phenomenon where particles become correlated in such a way that the state of one particle is dependent on the state of another, regardless of the distance between them. In a QET scenario, one system (the sender) is entangled with another system (the receiver). The sender is provided with energy. This energy is teleported to the receiver through the entangled connection without physically traversing the space between them.

Quantum energy teleportation has only been tested in bipartite systems [10] till now, leaving a broad scope of exploration for its behavior in multipartite systems. However, multipartite systems are complex. If one qubit is measured, then all of the entangled states will collapse. This is the case with Greenberger-Horne-Zeilinger (GHZ) state [11]. If we measure an arbitrary qubit from a multi-qubit system, the system collapses into a single state, and entanglement ceases to exist. Measuring any one of the qubits, therefore, destroys the multipartite entanglement.

However, a successful energy exchange among multiple parties entails that the entanglement is preserved between parties that have not yet been

3

measured. In contrast to the GHZ state, in the W state [12], all of the qubits are entangled, and the state is highly robust against single-particle measurements, meaning that the entanglement is preserved even if one of the qubits is lost or measured [13]. This serves our goal of preserving the state of the remaining subsystem when one of the particles is measured for harvesting energy. So, we created our circuit using W-state entanglement such that all the particles involved are entangled. For better visualization, figure 1a shows that four systems located at arbitrary distances are all entangled. Figure 1b shows that after injecting energy into one of the systems and making a measurement, the remaining subsystem remains thoroughly entangled.

3. Circuit Implementation

We have implemented several multi-qubit QET circuits incorporating multiqubit QET protocols as shown in figure 2, 3 and 4. The circuit in figure 2 uses three qubits where q0 is representative of Alice (the sender) while q1 and q2 are representative of Bob and Charlie, respectively (the receivers). At first, the particles are entangled using W-state entanglement. Then Alice deposits energy into her system and sends the information about her measured state to Bob or Charlie. Bob and Charlie can measure the energy in their subnetwork by passing the information sent by Alice to their unitary operators. Similarly, the circuit is extended for additional qubits using the same protocol. Figure 3 shows the circuit connection for four qubits, and figure 4 is for five qubits.

Our proposed architecture uses a reduced number of gates compared to the traditional implementation of W-state entanglement [14]. In doing so, it reduces the time complexity from linear $O(N)$ to logarithmic $O(log_2 N)$. So, our circuit is fast and optimized.

3.1. Preparing Entanglement

GHZ and W-state are classic representations of the general multipartite entanglement [15]. While GHZ is more fragile against loss, W-state is more robust against it [16]. W representation is central to quantum memories, multiparty quantum network protocols, and universal quantum cloning machines.

Another critical aspect of entanglement is that if one state is measured, all other states collapse. However, each receiver should be able to measure locally without collapsing the entanglement between other pairs. So, we used
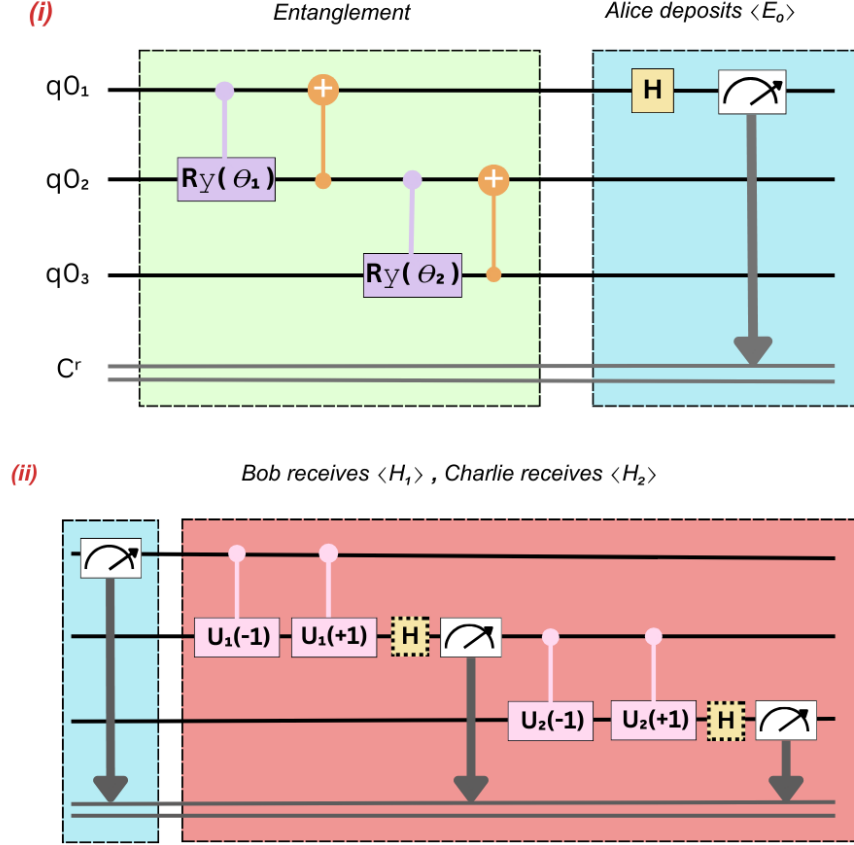
4

Figure 2: 3 qubit systems for quantum energy teleportation. Here, (i) represents the circuit portion where the subsystems are entangled. Immediately after entanglement, Alice deposits energy into the system through projective measurement. (ii) shows the part of the circuits where the measurement outcome is shared with the receivers, Bob and Charlie, via a classical channel.
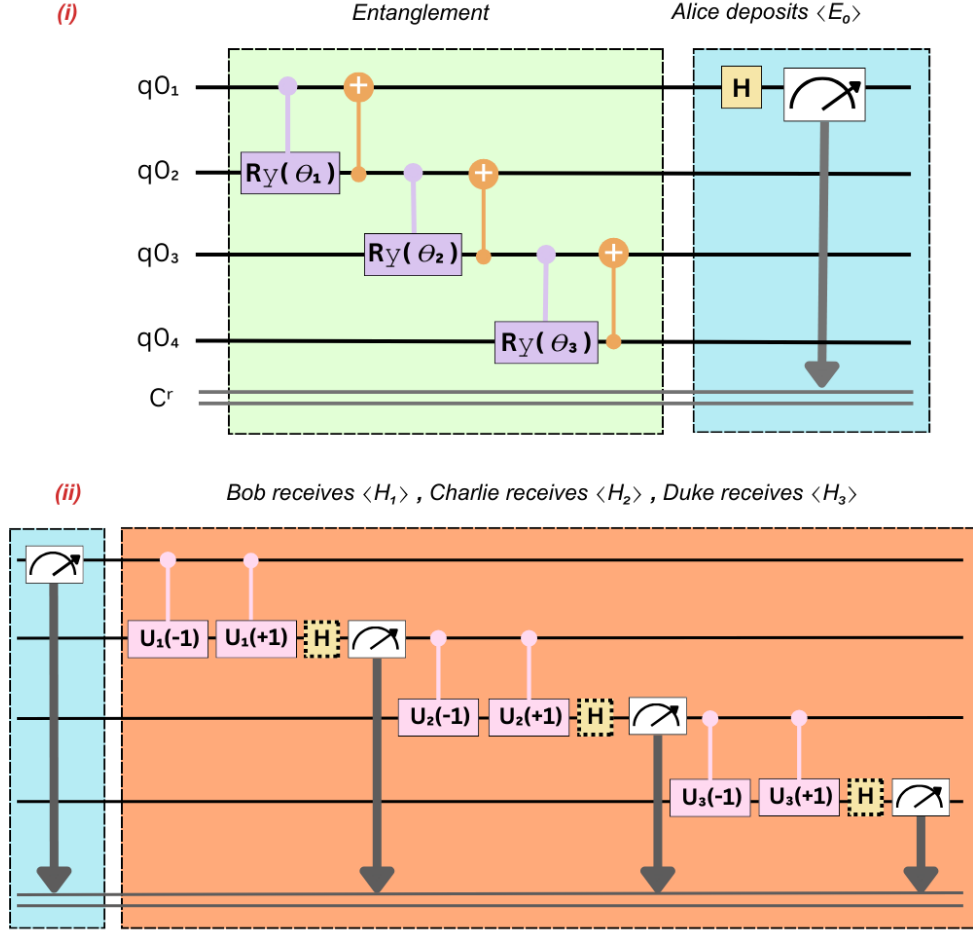
Figure 3: 4 qubit system for quantum energy teleportation. Here, (i) represents the circuit portion where the subsystems are entangled. Immediately after entanglement, Alice deposits energy into the system through projective measurement. (ii) shows the part of the circuits where the measurement outcome is shared with the receivers, Bob, Charlie, and Duke via a classical channel.
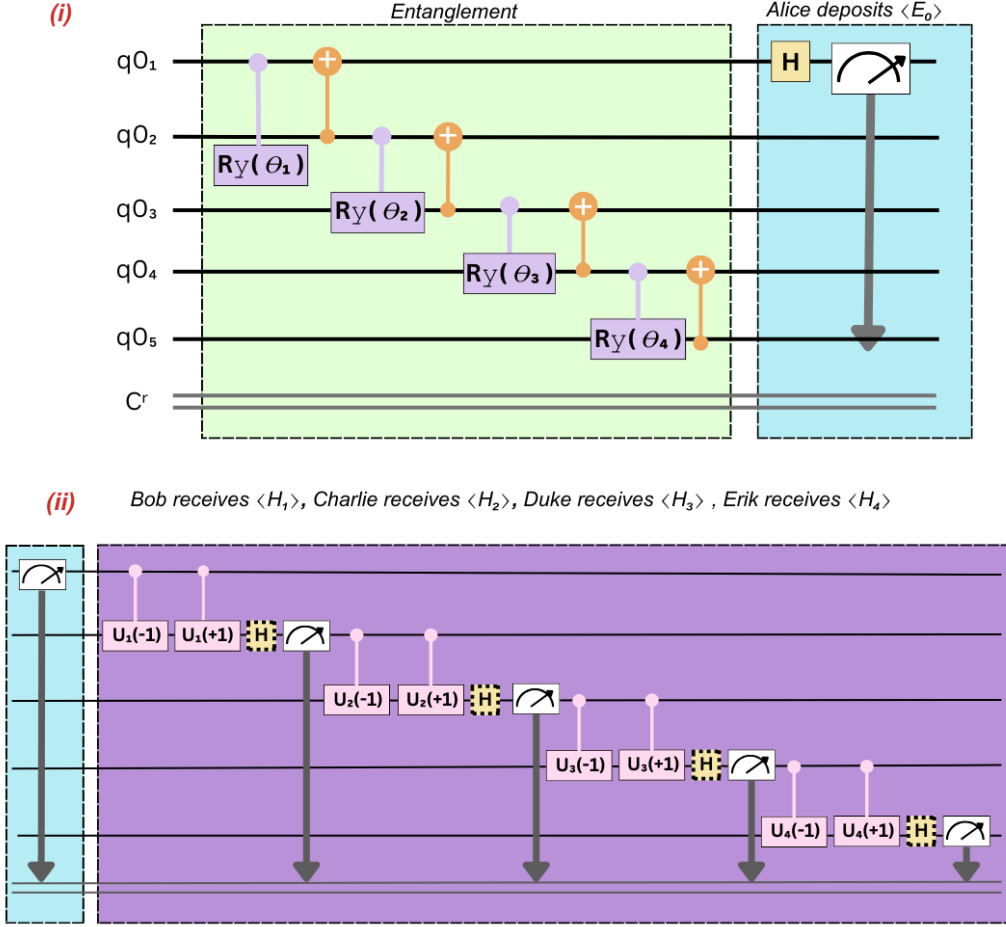
Figure 4: 5 qubit system for quantum energy teleportation. Here, (i) represents the circuit portion where the subsystems are entangled. Immediately after entanglement, Alice deposits energy into the system through projective measurement. (ii) shows the part of the circuits where the measurement outcome is shared with the receivers, Bob, Charlie, Duke, and Erik, via a classical channel.

a W-state entanglement between each pair to ensure that the measurement between one does not affect the other.

W-state [7] can be generalized for n qubits as shown in equation 1. An example of three qubits is mentioned in equation 2. Here, the quantum superposition exists with equal expansion coefficients for all possible pure states in which precisely one of the qubits is in an "excited state," whereas all others are in the "ground state."

$$|W_n\rangle = \frac{1}{\sqrt{n}}(|100...0\rangle + |010...0\rangle + ... + |00...01\rangle) \tag{1}$$

$$|W_3\rangle = \frac{1}{\sqrt{3}}(|100\rangle + |010\rangle + |001\rangle) \tag{2}$$

The robustness against particle loss and the LOCC-inequivalence with the (generalized) GHZ state also hold for the n-qubit W state. We have chosen the n-qubit W-state entanglement for our architecture to incorporate these advantages.

In this entanglement scenario, if the ground state is separable, the subsystems do not correlate. So, to teleport energy, we bring the systems to their ground states and create some ground-state entanglement [17]. Then, the entire system has zero-point energy. The total Hamiltonian of the system can be described by equation 3, where the Hamiltonians of each local system sum up to the total Hamiltonian.

$$H_{\text{total}} = \sum_{i=0}^{N-1} H_i + V \tag{3}$$

Each Hamiltonian may have its own substructure or components hosting multiple subsystems:

$$H_{\text{total}} = \sum_{i=0}^{m-1} H_i + H_{sub_m} + V, \tag{4}$$

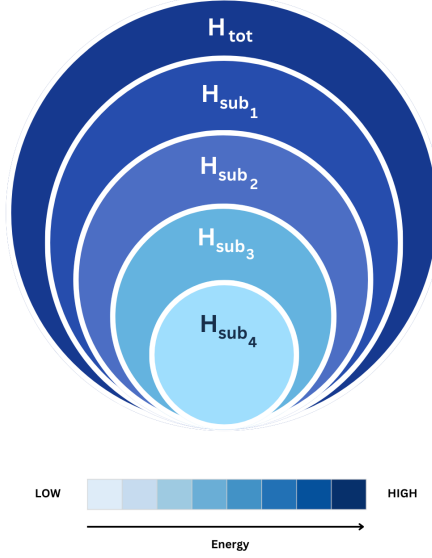$$H_{sub_m} = \sum_{i=m}^{N-1} H_i \tag{5}$$

8

Figure 5: Total Hamiltonian includes Hamiltonian of each subsystem. Again, each subsystem may also have substructures with Hamiltonians that sum up to the subsystem's total Hamiltonian.

3.2. Injecting Energy

Multiqubit QET is carried out in a quantum many-body system. It is known that any non-trivial local operations performed on a quantum many-body system give rise to excited states [18]. This includes measurements of the many-body's ground state, increasing the energy expectation value. So, in our experiment, the energy is injected into the sender's system by the experimental devices used for measurement. This projective measurement occurs with the following operation where μ is the outcome.

$$\sigma(\mu) = \frac{1}{2}(1 + \mu X_0). \tag{6}$$

Since the quantum many-body system is entangled [19], local injection of energy affects the global ground states, i.e., energy is supplied to the entire system [20]. However, the local injection occurred through measurement, destroying the entanglement between the two subsystems. The information about the injected energy is passed on to the entire system before this because the subsystems were already entangled. The measured outcome of the sender contains the information necessary to extract the energy from the subsystems.

9

After the W–state entangling gates are applied, the N–qubit register is brought to the *normalised* superposition

$$|\psi_{\text{init}}\rangle \;=\; \frac{k\,|0\cdots0\rangle \;+\; h\,|W_N\rangle}{\sqrt{h^2 + k^2}}, \qquad h, k \in \mathbb{R}_{\geq 0}. \tag{7}$$

The real parameters h and k tune the relative weight of the true vacuum and the single-excitation W_N component; they completely determine the energy that can be unlocked in the subsequent QET protocol.

The expectation value of the energy injected into the system is:

$$E_0 \;=\; \frac{h^2}{h^2 + k^2}. \tag{8}$$

Before injecting the energy, the entire system is brought to ground-point energy. At that point, the energy injected into the system is equivalent to the total Hamiltonian of the system.

$$H_{total} = E_0 \tag{9}$$

The entire system gains energy by injecting energy into one of the participants. The individual Hamiltonians incorporate this information.

$$H_n \;=\; |1\rangle_n\langle 1| \;=\; \frac{1}{2}\big(I - Z_n\big), \qquad n = 0, \ldots, N-1, \tag{10}$$

3.3. Classical Communication

Once the sender makes a measurement, the entanglement breaks, and there is a measurement outcome of either $\mu = -1$ or $+1$. This state information is then passed via a classical channel to the receivers, who can use this information to harvest the energy from their local systems. This information is sent as classical bits, and without this information, the receivers cannot obtain the target state. Because classical information needs to be sent, quantum teleportation cannot occur faster than the speed of light. After receiving the classical bit $\mu = \pm 1$, each receiver applies the conditional operation

$$U_\mu \;=\; \begin{cases} I, & \mu = +1, \\ Z, & \mu = -1, \end{cases}$$

on its own qubit. This implements σ_μ^{-1}, erases the μ-dependent phase, and converts the remote negative-energy pocket into a positive local excitation ready for harvesting.

3.4. Harvesting Energy

The post-measurement state $\sigma_\mu \, |\psi\rangle$ of the receiver's subsystem is different from its pre-measurement state $|\psi\rangle$. The receiver can only know this post-measurement state through the classical channel. Once Alice observes the state $\mu \in \{-1, 1\}$ using local measurement, she sends it to the receivers. When the information reaches the receivers, they can correct the state by performing a unitary operation σ_μ^{-1} on their subsystem. Then, the receivers are ready to perform local measurements on their subsystems to harvest the energy injected through entanglement in their ground states.

After measuring Alice's local energy, the entire system can be reimagined in terms of two subsystems where Alice is separated from the remaining entangled structure.

$$H_{total} = H_0 + H_{sub1} + V \tag{11}$$

where

$$H_{sub1} = H_1 + H_{sub2} \tag{12}$$

Similarly, after measuring Bob:

$$H_{total} = H_0 + H_1 + H_{sub_2} + V \tag{13}$$

Finally, for a three-qubit system, after measuring Charlie:

$$H_{total} = H_0 + H_1 + H_2 + V \tag{14}$$

Because all qubits are now in product states, the entangling interaction has vanished,

$$V \longrightarrow 0,$$

so that the final Hamiltonian is simply $H_{\text{total}} = \sum_{i=0}^{N-1} H_i$ with no residual coupling.

4. Symmetry Test

4.1. Translational Symmetry

Translational symmetry implies that a system's laws of physics, properties, and behavior remain unchanged under spatial translations or shifts. In simpler terms, it means that the physical properties of a system do not depend on its position in space. If we measure the total Hamiltonian of a
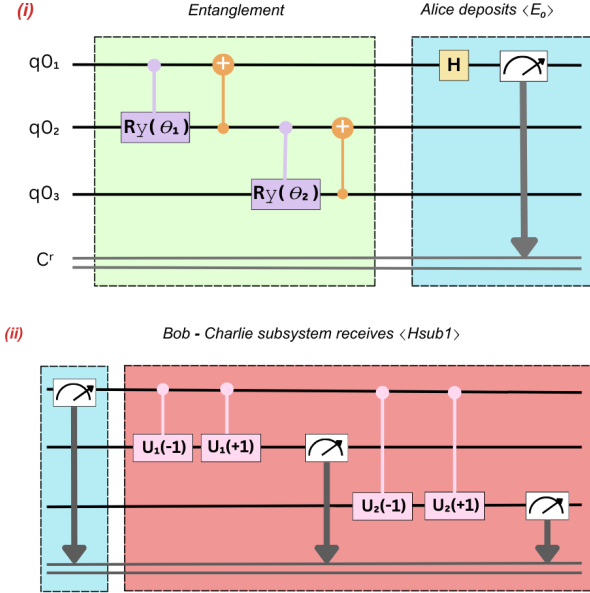
Figure 6: Translational Symmetry: The Hamiltonian of the subsystem measured from any of its nodes gives the same result.

subsystem, then it must be the same from any subsystem node. Figure 6 shows our circuit design for testing this. After measuring Alice's energy, the remaining subsystem has a Hamiltonian of H_{sub_1}, which is measured to be the same from any node of the subsystem. So, our design passes the test.

4.2. Exchange Symmetry

Exchange symmetry refers to the principle that identical particles cannot be distinguished from one another. If you have two identical particles and exchange their positions in a system, the system's properties should remain unchanged. Figure 7 shows the circuit design where the third qubit (Charlie) is measured before the second qubit (Bob). The measurement outcomes remain unchanged even after exchanging the order.

$$\psi(A, B) = \psi(B, A) \tag{15}$$

5. Results Analysis

The energy readings obtained from our QET experiment across multi-qubit systems unveil some exciting patterns. For a three-qubit system, Table
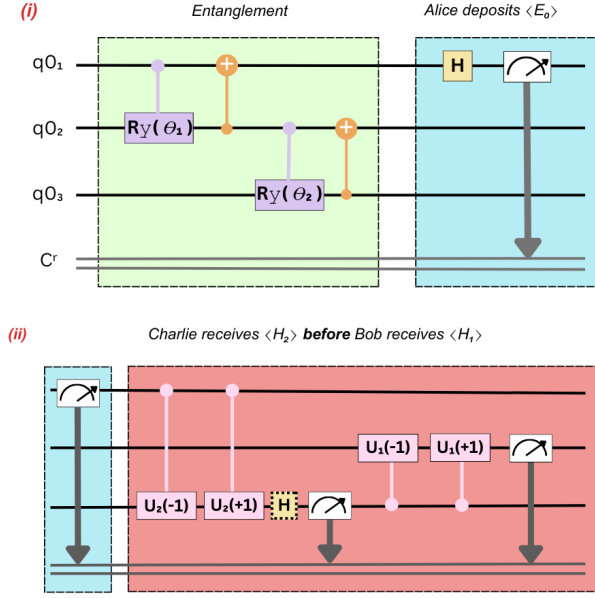
Figure 7: Exchange Symmetry: Charlie and Bob switch order of measurement.

1 shows that the energy readings obtained by measuring the qubits gradually decrease according to who measures first. This is because each Hamiltonian incorporates the Hamiltonians of their substructures. Similarly, Table 2 and 3 demonstrate 4 and 5 qubit systems. The graphical representation of the combined values from Table 1, 2, and 3 is seen in Figure 8. Both Figure 8a and 8b show the gradual decrement of the Hamiltonians of the subsystems for qasm_simulator and real device, respectively. It is essential to understand that the readings are not for a particular qubit but for the entangled substructure. These substructures contain several qubits with individual Hamiltonians. So, the energy the sender initially injects is first distributed into the entire system. Then, the share of individual qubits is learned through measurement. The sum of the individual qubit energies never exceeds the amount of injected energy. There is conservation of energy. Some energy injected into the system is lost, and the remaining is dispersed throughout the system. We recorded the energy measurements in both simulation and real quantum devices. In both platforms, the same relation exists where the injected energy is distributed from the sender to the entire system, and the subsystems contain the energy in a decremental order followed by measurement. This is because in W-state entanglement, even after the measurement

13
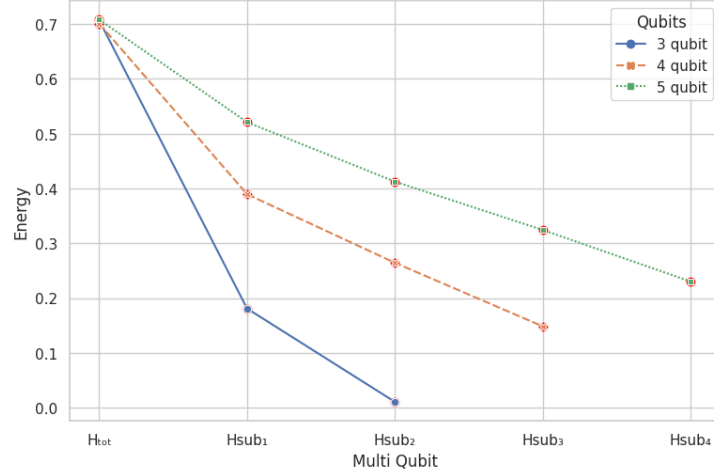
(a) Simulation(qasm-simulator)
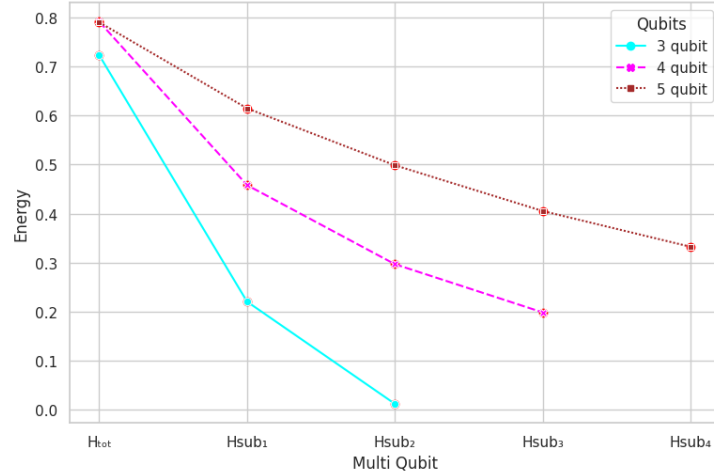
(b) Real Quantum Device (ibm_lagos)

Figure 8: The energy readings from each subsystem in the multi-qubit system show a decremental energy distribution.

of a qubit, only the entanglement between that qubit and others is reduced to a single state, whereas all other qubits remain entangled. So, the remaining entangled subsystem has energy dispersed within its network. The same scenario exists across all of the multiqubit systems as shown in Table 1, 2, 3, and figure 8.
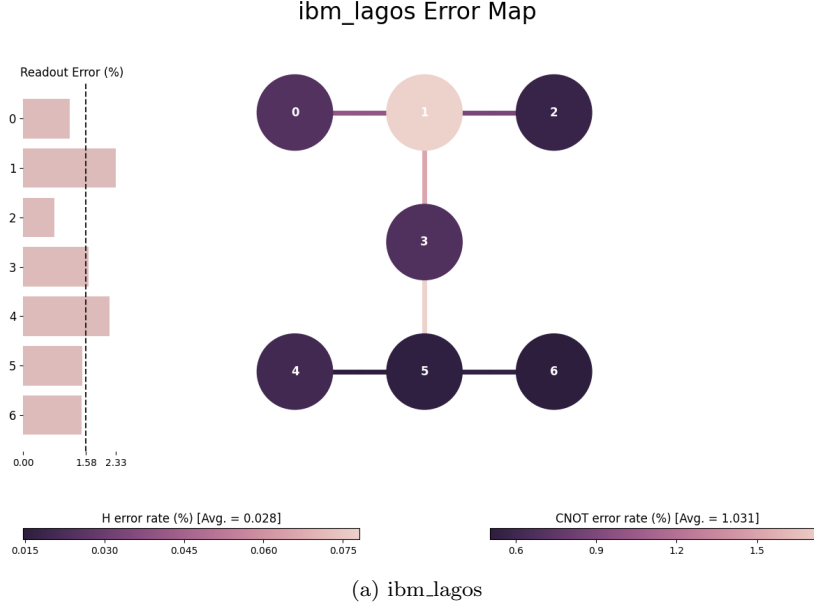
(a) ibm_lagos

Figure 9: Error Map

6. Real Quantum Device

Our study was not limited to simulation only. We have run extensive experimentation on real quantum computers provided by IBM, which anyone can access. The device available to us was IBMQ Lagos. Figure 9 shows the error maps of these devices, which represent the error rates associated with the various quantum gates and operations performed on the quantum processor. It is crucial to characterize and understand the errors that occur during the execution of quantum circuits. This is because these errors can limit the performance and reliability of quantum algorithms. Despite these challenges, real quantum devices provide valuable insights into the practical limitations and opportunities for quantum computing, and simulations remain important tools for algorithm development and benchmarking. The comparisons between the simulation values and real values in Table 1, 2, and 3 shed some light on how real device noise makes the readings slightly different from the simulation. However, due to the simplified architecture used in this study, we observed a noticeably low error deviation rate even with a higher circuit depth.

Our setup has no significant deviation of results from real quantum de-

vices, so our multiqubit energy teleportation system is feasible for real-world applications. The proposed multiqubit QET protocol stands robust against real-world quantum device limitations. With additional error-mitigation strategies the accuracy could be further improved [21].

7. Conclusion

We have presented the first experimental realisation of *multi-qubit* quantum-energy teleportation (QET) using a robust W-state architecture. Our three-, four-, and five-qubit circuits were executed both in noiseless simulation and on the `IBMQ Lagos` superconducting processor, demonstrating that a single sender can inject an energy E_0 that is then *deterministically and decrementally* harvested by multiple, spatially separated receivers. Energy conservation and causality are respected throughout: the sum of all harvested energies never exceeds E_0, and classical feed-forward limits the protocol to light-speed signalling.

Two internal consistency checks—translational symmetry of the residual sub-Hamiltonian and exchange symmetry under permutation of receiver order—were passed on both the simulator and hardware runs, confirming that the observed distribution pattern is an intrinsic feature of the W-state QET protocol.

The present proof-of-principle is limited by NISQ-era (noisy intermediate-scale quantum) noise and by the single-excitation nature of the W state, so only a fraction of the injected energy is ultimately recovered. Nevertheless, today's quantum hardware is already powerful enough to implement and verify the protocol up to five qubits, and error-mitigation techniques promise even higher fidelity.

Looking forward, larger entangled networks, alternative resource states, and hybrid photonic-superconducting platforms could enable long-range energy distribution or even probing topological order via QET spectroscopy. Our results therefore open a practical path toward energy-aware quantum networks and deepen the link between entanglement, information and thermodynamics.

Table 1: Energy readings from QET experiment for three qubits. E_0 is the energy injected, H_n is the hamiltonian of the nth qubit and H_{sub_n} is the hamiltonian of the nth subsystem where $H_{sub_m} = \sum_{i=m}^{N-1} H_i$.

Energy	h, k	qasm simulator	*IBMQLagos*
H_{tot}	2,1	1.7845 ± 0.0063	1.8627 ± 0.0063
	1,1	0.7064 ± 0.0031	0.7321 ± 0.0031
H_{sub_1}	2,1	0.7314 ± 0.0053	0.9611 ± 0.0057
	1,1	0.1809 ± 0.0026	0.2206 ± 0.0028
H_{sub_2}	2,1	0.3918 ± 0.0045	0.4675 ± 0.0058
	1,1	0.0107 ± 0.0022	0.0122 ± 0.0028
E_o	2,1	1.7888	1.7888
	1,1	0.7071	0.7071
H_1	2,1	1.0531	0.9016
	1,1	0.5255	0.5115
H_2	2,1	0.3396	0.4936
	1,1	0.1702	0.2084

Table 2: Energy readings from QET experiment for four qubits. E_0 is the energy injected, H_n is the hamiltonian of the nth qubit and H_{sub_n} is the hamiltonian of the nth subsystem where $H_{sub_m} = \sum_{i=m}^{N-1} H_i$.

Energy	h, k	qasm simulator	*IBMQLagos*
H_{tot}	2,1	1.7846 ± 0.0063	1.9186 ± 0.0063
	1,1	0.7009 ± 0.0031	0.7915 ± 0.0031
H_{sub_1}	2,1	1.1575 ± 0.0060	1.4426 ± 0.0062
	1,1	0.3895 ± 0.0029	0.4582 ± 0.0031
H_{sub_2}	2,1	0.9156 ± 0.0056	1.0287 ± 0.0061
	1,1	0.2644 ± 0.0028	0.2970 ± 0.0030
H_{sub_3}	2,1	0.6624 ± 0.0052	0.7885 ± 0.0060
	1,1	0.1485 ± 0.0026	0.1987 ± 0.0031
E_o	2,1	1.7888	1.7888
	1,1	0.7071	0.7071
H_1	2,1	0.6271	0.476
	1,1	0.3114	0.3333
H_2	2,1	0.2419	0.4139
	1,1	0.1251	0.1612
H_3	2,1	0.2532	0.2402
	1,1	0.1157	0.0983

Table 3: Energy readings from QET experiment for five qubits. E_0 is the energy injected, H_n is the hamiltonian of the nth qubit and H_{sub_n} is the hamiltonian of the nth subsystem where $H_{sub_m} = \sum_{i=m}^{N-1} H_i$.

Energy	h, k	qasm simulator	$IBMQLagos$
H_{tot}	2,1	1.7830 ± 0.0063	1.9488 ± 0.0063
	1,1	0.7079 ± 0.0031	0.7902 ± 0.0031
H_{sub_1}	2,1	1.4128 ± 0.0062	1.77989 ± 0.0063
	1,1	0.5210 ± 0.0031	0.6148 ± 0.0031
H_{sub_2}	2,1	1.2120 ± 0.0060	1.4866 ± 0.0063
	1,1	0.4125 ± 0.0030	0.4987 ± 0.0031
H_{sub_3}	2,1	1.0266 ± 0.0058	1.2777 ± 0.0063
	1,1	0.3243 ± 0.0029	0.4054 ± 0.0031
H_{sub_4}	2,1	0.8325 ± 0.0055	1.0973 ± 0.0063
	1,1	0.2303 ± 0.0027	0.3325 ± 0.0031
E_o	2,1	1.7888	1.7888
	1,1	0.7071	0.7071
H_1	2,1	0.3702	0.169
	1,1	0.1869	0.1754
H_2	2,1	0.2008	0.2932
	1,1	0.1085	0.1161
H_3	2,1	0.1854	0.2089
	1,1	0.0882	0.0933
H_4	2,1	0.1941	0.1797
	1,1	0.094	0.0729

References

[1] Masahiro Hotta, Jiro Matsumoto, and Go Yusa. Quantum energy teleportation without a limit of distance. *Physical Review A*, 89(1):012311, 2014.

[2] Masahiro Hotta. Quantum energy teleportation: an introductory review. *arXiv preprint arXiv:1101.3954*, 2011.

[3] Masahiro Hotta. Quantum energy teleportation in spin chain systems. *Journal of the Physical Society of Japan*, 78(3):034001, 2009.

[4] Kazuki Ikeda and others. Demonstration of quantum energy teleportation on superconducting quantum hardware. *Physical Review Applied*, 20(2):024051, 2023.

[5] Kazuki Ikeda. First realization of quantum energy teleportation on quantum hardware. *arXiv preprint arXiv:2301.02666*, 2023.

[6] Charles H. Bennett, Gilles Brassard, Claude Crépeau, Richard Jozsa, Asher Peres, and William K. Wootters. Teleporting an unknown quantum state via dual classical and Einstein-Podolsky-Rosen channels. *Physical Review Letters*, 70(13):1895, 1993.

[7] Ya-Hong Wang and He-Shan Song. Preparation of partially entangled W state and deterministic multi-controlled teleportation. *Optics Communications*, 281(3):489–493, 2008.

[8] Eric Chitambar, Debbie Leung, Laura Mančinska, Maris Ozols, and Andreas Winter. Everything you always wanted to know about LOCC (but were afraid to ask). *Communications in Mathematical Physics*, 328:303–326, 2014.

[9] Jeffrey Bub. Quantum entanglement and information. *2001*.

[10] L.-A. Wu, Marcelo S. Sarandy, and D. A. Lidar. Quantum phase transitions and bipartite entanglement. *Physical Review Letters*, 93(25):250404, 2004.

[11] Rajiuddin Sk, Tadasha Dash, and Prasanta K. Panigrahi. Quantum information splitting of an arbitrary three-qubit state by using three sets of GHZ states. *IET Quantum Communication*, 2(3):122–135, 2021.

[12] Wolfgang Dür, Guifre Vidal, and J. Ignacio Cirac. Three qubits can be entangled in two inequivalent ways. *Physical Review A*, 62(6):062314, 2000.

[13] Xue-Ping Zang, Ming Yang, Fatih Ozaydin, Wei Song, and Zhuo-Liang Cao. Generating multi-atom entangled W states via light-matter interface based fusion mechanism. *Scientific Reports*, 5(1):16245, 2015.

[14] Diogo Cruz, Romain Fournier, Fabien Gremion, Alix Jeannerot, Kenichi Komagata, Tara Tosic, Jarla Thiesbrummel, Chun Lam Chan, Nicolas Macris, Marc-André Dupertuis, and others. Efficient quantum algorithms for GHZ and W states, and implementation on the IBM quantum computer. *Advanced Quantum Technologies*, 2(5-6):1900015, 2019.

[15] Bob Coecke and Aleks Kissinger. The compositional structure of multipartite quantum entanglement. *arXiv preprint arXiv:1002.2540*, 2010.

[16] Ellie D'Hondt and Prakash Panangaden. The computational power of the W and GHZ states. *arXiv preprint quant-ph/0412177*, 2006.

[17] Masahiro Hotta. Ground-state entanglement gives birth to quantum energy teleportation. In *Quantum Communication and Quantum Networking: First International Conference, QuantumComm 2009, Naples, Italy, October 26-30, 2009, Revised Selected Papers 1*, pages 66–73. Springer, 2010.

[18] Shuo Liu, Shi-Xin Zhang, Chang-Yu Hsieh, Shengyu Zhang, and Hong Yao. Probing many-body localization by excited-state variational quantum eigensolver. *Physical Review B*, 107(2):024204, 2023.

[19] Luigi Amico, Rosario Fazio, Andreas Osterloh, and Vlatko Vedral. Entanglement in many-body systems. *Reviews of Modern Physics*, 80(2):517, 2008.

[20] Masahiro Hotta. Energy entanglement relation for quantum energy teleportation. *Physics Letters A*, 374(34):3416–3421, 2010.

[21] Ryuji Takagi, Suguru Endo, Shintaro Minagawa, and Mile Gu. Fundamental limits of quantum error mitigation. *npj Quantum Information*, 8(1):114, 2022.